Transcription dynamics stabilizes nucleus-like layer structure in chromatin brush†

Tetsuya Yamamoto [iD] ‡*[a] and Helmut Schiessel§[ab]

We use a brush of DNA in a solution of transcriptional machinery and histone proteins to theoretically predict that this brush shows phase separation due to the instability arising from the disassembly of nucleosomes during transcription. In the two-phase coexistent state, collapsed chains (with relatively large nucleosome occupancy) lie at the grafting surface and swollen chains (with relatively small nucleosome occupancy) are distributed at the space above the collapsed chains, analogous to the structure of chromatin in differentiated cells. This layer structure is stabilized by the lateral osmotic pressure of swollen chains. For a relatively small grafting density, DNA brushes show tricritical points because the entropic elasticity with respect to the lateral excursion of swollen chains balances with the lateral osmotic pressure of these chains. At the tricritical points, DNA brushes show large fluctuations of local nucleosome concentration, which may be reminiscent of the fluctuations observed in embryonic stem cells.

1 Introduction

In an eukaryotic cell DNA is packed in a nucleus as chromatin, a complex of DNA and histone proteins.[1] The repeating unit of chromatin is the nucleosome, in which DNA is wound around an octamer of histone proteins by 1.65 turns.[2] The chromatin of embryonic stem (ES) cells shows fluctuations in nucleosome density of relatively long time (in the order of minutes) and length (in the order of μm) scales, analogous to critical fluctuations.[3] In contrast, chromatin of differentiated cells shows regions of relatively large nucleosome density (which are called heterochromatin) that coexist with regions of relatively small nucleosome density (which are called euchromatin). In many differentiated cells, heterochromatin is localized at the vicinity of nuclear membranes and euchromatin is localized at the center of the nucleus (which we call the canonical structure). The transitions of chromatin structures during differentiation are reminiscent of phase separation. Because the rate with which a stretch of DNA is transcribed depends on the local packing density of nucleosomes, the phase separation of chromatin during differentiation may play an important role in determining the lineage of stem cells. It is thus of interest to theoretically study the physics of the phase separation and pattern formation of chromatin.

The classical theory of phase separation predicts that the phase separation is driven by the attractive interactions between nucleosomes (that stabilize the condensed state, where local nucleosome concentrations are relatively large) and thermal fluctuations (that destabilize the condensed state).[12] Nucleosomes show attractive interactions at physiological salt concentrations because overall positively charged histone tails bind to the cores of other nucleosomes, which are negatively charged due to the charge inversion.[13–16] However, nucleosomes are relatively stable structures and thermal fluctuations are not large enough to disassemble nucleosomes and/or drive thermal diffusion of nucleosomes along DNA.[17–19] Single molecule experiments have shown that nucleosomes are disassembled when RNA polymerase (RNAP) collides with nucleosomes during transcription.[20,21] This process may thus break the symmetry of chromatin and drive the phase separation. Indeed, a comparison between theory and experiments suggest that fluctuations arising from active processes dominate thermal fluctuations for long time scales.[22]

A DNA brush, in which DNA is end-grafted to a solid surface, is a simple model system, which enables us to quantitatively change the local packing density of DNA.[4–11] When a DNA brush is prepared in a solution of histone proteins, one can also control the local concentration of nucleosomes in the brush *via* the grafting density of DNA and the concentration of histone proteins in the solution. DNA brushes may be thus useful to study the physics of the phase separation and pattern formation of chromatin. In our previous work, we have theoretically predicted that a DNA brush shows phase separation in a solution of transcription machinery and histone proteins.[11] Our theory

[a] *Department of Materials Physics, Nagoya University, Furocho, Chikusa-ku, Nagoya, 464-8603, Japan. E-mail: tyamamoto@nuap.nagoya-u.ac.jp*

[b] *Instituut-Lorentz for Theoretical Physics, Niels Bohrweg 2, Leiden, 2333 CA, The Netherlands*

predicts that this phase separation is driven by an instability arising from the fact that the nucleosome occupancy of DNA chains decreases with increasing the transcription rate on these chains due to the collision between RNAP and nucleosomes during transcription; the transcription rate, in turn, further increases with decreasing the nucleosome occupancy because the local concentration of RNAP is larger at a region of smaller nucleosome concentration due to the excluded volume interactions between RNAP and nucleosomes. However, this theory is effective only for cases in which DNA brushes show macroscopic lateral phase separation.

Mixed polymer brushes show various patterns of microphase separation.[23–26] Recently, van Lehn and Alexander-Katz have theoretically predicted that two-component polymer brushes show various patterns of domains, for cases in which the molecular weights of miscible polymers are very different, due to the lateral osmotic pressure of longer chains.[23] The tendency of such a brush to suppress macroscopic phase separation, even when the grafting-ends of the constituent polymers are mobile along the surface, was first predicted by Komura and Safran.[27] Motivated by these results, we present here an extension of our previous theory of DNA brushes[11] to predict the structures of these brushes in the two-phase coexistent state. We find that in the two-phase coexistent state, DNA brushes form a layer structure, in which DNA chains of larger nucleosome occupancy collapse on the grafting surfaces and DNA chains of smaller nucleosome occupancy cover the space above the collapsed chains. This structure is stabilized by the lateral osmotic pressure of the swollen chains. For a relatively small grafting density, DNA brushes show a tricritical point, where the fraction of swollen chains fluctuates significantly. This is because the lateral osmotic pressure is balanced by the entropic elasticity with respect to the lateral excursions of swollen chains. This situation is very different from the two-component polymer brushes, where the fraction of polymer components is fixed. The layer structure is reminiscent of the canonical structure of differentiated cell nuclei and the fluctuations at the tricritical point are reminiscent of chromatin dynamics in ES cells. Our theory may provide insight into the physics of the phase separation of chromatin during differentiation.

2 Methods

2.1 DNA brush

We take into account the possibility of stabilizing layer structures in an extension of our previous model.[9,11] We treat a DNA brush, where DNA chains are end-grafted to a surface with a grafting density σ (see Fig. 1). Each DNA chain is composed of N chain segments of length l_{eff}. We treat these DNA chains as a 1d lattice of binding sites, which can be occupied by nucleosomes or RNAP. For simplicity, we assume that each chain segment has one binding site, although one Kuhn segment of DNA chain ($\sim$100 nm) is long enough to assemble two nucleosomes. Each DNA chain has a promoter (transcription starting site) at one end and a terminator (transcription ending site) at the other end.
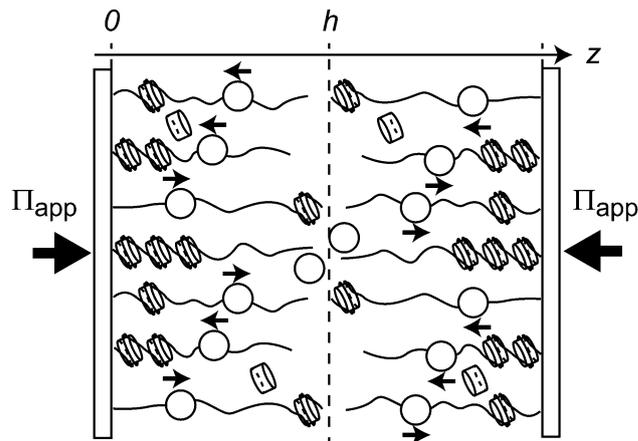

Fig. 1 Homogeneous DNA brushes are prepared by end-grafting DNA chains on a surface. These DNA brushes are in a solution of RNA polymerase (shown as spheres), histone proteins (shown as cylinders), and other small molecules that are necessary for transcription and nucleosome assembly. Pressure is applied to a DNA brush by pushing it to another symmetric DNA brush. We use the coordinate systems, where the z-direction is normal to the grafting surface. [Reproduced from ref. 11.]

DNA chains that are end-grafted at the promoter end are randomly mixed with DNA chains that are end-grafted at the terminator ends. The DNA brush is in a solution of RNAP and histone proteins (and other small molecules that are necessary for transcription and the assembly of nucleosomes). We use the Alexander approximation, where the concentration of DNA chain segments is assumed to be uniform in the brush region (in the z-direction). With this approximation, the promoters and terminators are located at the brush top and grafting surface.

2.2 Transcription dynamics

The nucleosome occupancy of DNA chains is derived by analyzing the transcription dynamics and the dynamics of nucleosome assembly and disassembly. We here treat the uni-directional motion of RNAP during transcription. Transcription starts when a RNAP binds to the promoter of a DNA chain. Then, the enzyme shows a uni-directional motion towards the terminator in a base-by-base manner, while synthesizing a RNA chain of complementary base sequence. When the RNAP reaches the terminator, it is released from the DNA chain, together with the RNA product. For simplicity, we do not treat here the stochasticity involved in the binding of RNAP to the promoters and in the uni-directional motion of RNAP along DNA.

The binding rate of RNAP to a promoter has the form

$$R_P = \lambda_P \rho, \qquad (1)$$

where ρ is the local concentration of RNAP at the position of the promoter (in the solution) and λ_P is the rate constant that accounts for the binding of RNAP to the promoter. We neglect the unbinding rate of RNAP from promoters because RNAP firmly grips DNA chains once it changes its conformation. The migration rate of RNAP along a DNA chain has the form

$$R_{uni} = \xi n_{rnp}(1 - n_{his}), \qquad (2)$$

where ξ is the rate constant that accounts for the motion of RNAP from one binding site to the next. The rate constant ξ is the inverse of the ensemble average of the total time, with which an RNAP moves by one Kuhn length, ~ 294 bp. We thus assume that the rate constant ξ is uniform along DNA chains. n_{rnp} is the occupancy of RNAP at one binding site and n_{his} is the nucleosome occupancy (the probability of finding a histone octamer) at the next binding site; eqn (2) shows the fact that the uni-directional motion of RNAP is hampered by nucleosomes. In steady states, n_{rnp} and n_{his} are uniform along DNA chains due to the Alexander approximation (see also Section 2.3). The unbinding rate of RNAP from the terminator has the form

$$R_t = \lambda_t n_{rnp}^t, \tag{3}$$

where λ_t is the rate constant that accounts for this process and n_{rnp}^t is the occupancy of RNAP at the terminator. With the forms of eqn (1) and (3), we assumed that the promoters and the terminators are not occupied by nucleosomes due to their specific basepair sequence. There is indeed nucleosome depletion at the transcription starting and ending sites.[28]

2.3 Dynamics of nucleosome assembly and disassembly

The local concentration of histone proteins is uniform in the brush region due to the Alexander approximation. Moreover, because histone proteins are smaller than RNAP, for simplicity, we neglect the interactions between histone proteins and nucleosomes (or vacant DNA chain segments). With this approximation the local concentration of histone proteins in the brush region is equal to the concentration c_0 of histone proteins in the external solution (defined by the chemical potentials of histone proteins). Without changing the physics, we neglected (i) the fact that nucleosome cores are composed of octamers of histone proteins, (ii) the specific chemistry of four types of histone proteins, and (iii) the fact that the assembly of nucleosomes are usually guided by chaperones.

The rate of nucleosome assembly has the form

$$R_{on} = \lambda_{his} c_0 (1 - n_{his}), \tag{4}$$

where λ_{his} is the rate constant that accounts for the assembly of nucleosomes. The rate of nucleosome disassembly has the form

$$R_{off} = \zeta n_{his} n_{rnp}. \tag{5}$$

With eqn (5), we neglected the spontaneous disassembly of nucleosomes due to thermal fluctuations. This equation represents the fact that nucleosomes are disassembled by the collision between RNAP and nucleosomes during transcription. ζ is the rate constant that accounts for this process.

2.4 Steady state

In steady states, the binding rate of RNAP at the promoter, the migration rate of RNAP along a DNA chain, and the unbinding rate of RNAP from the terminator are all equal. The rates of nucleosome assembly and disassembly are also equal. These equalities have the forms

$$R_p = R_{uni}(= R_t) \tag{6}$$

$$R_{on} = R_{off} \tag{7}$$

These equalities lead to the nucleosome occupancy n_{his} as a function of the local concentration ρ of RNAP at the position of the promotor (in the solution) and the rate constants.

With the local equilibrium approximation, the chemical potential μ_{rnp} of RNAP is continuous at the brush top. Because DNA chains are end-grafted with random orientations, the transcription dynamics along these DNA chains does not generate gradients of RNAP concentrations; the chemical potential μ_{rnp} is uniform in the entire system. The local concentration of RNAP in the brush region thus has the form

$$\rho = \rho_0 e^{-\nu \Phi_{on}}, \tag{8}$$

where ν is the 2nd virial coefficient that accounts for the interactions between nucleosomes and RNAP. ρ_0 is the concentration of RNAP in the external solution (defined by the chemical potential μ_{rnp} of RNAP). Φ_{on} is the local concentrations of nucleosomes in the brush region that have the form

$$\Phi_{on} = \frac{\sigma N}{h} n_{his}, \tag{9}$$

where h is the height of the brush. Eqn (6)–(8) lead to the nucleosome occupancy as a function of brush height.

2.5 Force balance equation

We treat cases in which a DNA brush is pushed into another DNA brush with applied pressure Π_{app}. In physiological salt concentrations, DNA chains are treated as electrically neutral semiflexible polymers of Kuhn length l_{eff}.[29] We here treat cases in which the dynamics of DNA chains is faster than the other dynamical processes mentioned above and thus the height of the brush is determined by the balance of forces. When DNA chains are much longer than the Kuhn length l_{eff}, the force balance equation of the brush in the z-direction has the form

$$\frac{\Pi_{app}}{T} = -\frac{3\sigma h}{N l_{eff}^2} + \frac{1}{2} w_{on} \Phi_{on}^2 + w_{int} \Phi_{on} \Phi_{off} + \frac{1}{2} w_{off} \Phi_{off}^2 + \frac{2}{3} u \Phi_{on}^3. \tag{10}$$

The first term on the right side of the equation is the entropic elasticity of DNA chains. The next three terms are the osmotic pressure arising from the (2-body) interactions between DNA chain segments. The last term is the osmotic pressure arising from the three-body interactions between nucleosomes and suppresses the complete collapses of DNA chains. To derive eqn (10), we used the fact that the osmotic pressure generated by RNAP and the interactions between RNAP and DNA chain segments do not change the structure of the brush for cases in which the concentration of RNAP is dilute enough. The Kuhn length has the form $l_{eff} = l_a (1 - \gamma n_{his})$, where l_a is the Kuhn length of vacant DNA chains (~ 100 nm) and γ is a constant that accounts for the fact that DNA chains are reeled around histone octamers when they assemble into nucleosomes. w_{on}, w_{int}, and w_{off} are the 2nd virial coefficients that account for the (nucleosome)–(nucleosome) interactions, the (nucleosome)–(vacant DNA segment) interactions, and the (vacant DNA segment)–(vacant DNA segment) interactions, respectively. Experiments have shown that the (vacant DNA segment)–(vacant DNA segment)

interactions are repulsive, $w_{\text{off}} > 0$, and the (nucleosome)–(nucleosome) interactions are attractive, $w_{\text{on}} < 0$, at physiological salt concentrations.[13–16] u is the virial coefficient that accounts for the 3-body interactions between nucleosomes. Because the fifth term is significant only for $n_{\text{his}} \sim 1$, we use the approximation $u\Phi_{\text{on}}{}^3 \simeq u\sigma^3 N^3/h^3$ throughout the paper. The local concentration Φ_{off} of vacant DNA chain segments has the form

$$\Phi_{\text{off}} = \frac{\sigma N}{h}(1 - n_{\text{his}}). \qquad (11)$$

Solving eqn (6), (7) and (10) leads to the nucleosome occupancy as a function of applied pressure, virial coefficients, and rate constants.

2.6 Maxwell construction and its extension

Eqn (6), (7) and (10) predict that applied pressure is a non-monotonic function of the height of the DNA brush, analogous to the van der Waals theory of liquid–gas phase transitions (see also Fig. 3). In the classical theory of phase separation, the binodal curves of the phase separation during the latter transitions are predicted by using the common tangent method.[12] This method is derived by the minimization of the free energy and may not be applicable to predicting the coexistence of two non-equilibrium steady states. The Maxwell construction is another method to predict the binodal curves and it ensures that the mechanical work to change one phase to the other coexisting phase is zero.[30] Steady state thermodynamics states that the difference of the generalized free energy between two non-equilibrium steady states is equal to the mechanical work that is necessary to change one state to the other.[31] Indeed, the mechanical balance at the interface between domains leads to the fact that the Maxwell construction is the necessary condition for two macroscopic phases to coexist (see also Section S1 in ESI†). Motivated by this result, we use an extension of the Maxwell construction to predict the transcription driven phase separation of DNA brushes.

We take into account the possibility of stabilizing a layer structure in an extension of the Maxwell construction. In contrast to two-component polymer brushes, the fraction ϕ of swollen chains in DNA brushes is not fixed and depends on the dynamics of nucleosome assembly and disassembly. To predict the fraction ϕ, we think of a two-step process where (i) pressure is applied to a fraction of chains in the normal direction to collapse chains and then (ii) swollen chains are allowed to diffuse to the space above the collapsed chains (see Fig. 2). The mechanical work that is necessary for this process has the form

$$W(\phi) = W_\perp(\phi) + W_\|(\phi) + W_{\text{int}}(\phi). \qquad (12)$$

The work $W_\perp(\phi)$ is necessary for the first step and $W_\|(\phi)$ is necessary for the second step. $W_{\text{int}}(\phi)$ is the work that is necessary to make interfaces between swollen chains and collapsed chains during the two steps. For simplicity, we neglect the interfacial work $W_{\text{int}}(\phi)$ in the main article, see Section S5 of the ESI.†

The work $W_\perp(\phi)$ done by the excess normal pressure has the form

$$W_\perp(\phi) = -(1 - \phi)A\int_{h_{\text{s}}^* + h_{\text{c}}}^{h_{\text{c}}} dh' \Pi_\perp(h'), \qquad (13)$$

where A is the area of the brush and ϕ is the fraction of swollen chains. h_{c} and $h_{\text{s}}^* + h_{\text{c}}$ are the height of collapsed and swollen chains and are two stable solutions of eqn (10) for a given applied pressure (see also Fig. 2a and b). The excess normal pressure $\Pi_\perp$ has the form

$$\frac{\Pi_\perp(h)}{T} = -\frac{3\sigma h}{N l_{\text{eff}}{}^2} + \frac{1}{2}w_{\text{on}}\Phi_{\text{on}}{}^2 + w_{\text{int}}\Phi_{\text{on}}\Phi_{\text{off}} + \frac{1}{2}w_{\text{off}}\Phi_{\text{off}}{}^2 \\ + \frac{2}{3}u\Phi_{\text{on}}{}^3 - \frac{\Pi_{\text{app}}}{T}, \qquad (14)$$

see also eqn (10). The work $W_\|(\phi)$ done by the excess lateral pressure has the form

$$W_\|(\phi) = -\int_{\phi A}^{A} dA' \Pi_\| h_{\text{s}}(A') + \int_{h_{\text{s}}^*}^{h_{\text{s}}(\phi)} dh_{\text{s}}' \Pi_{\text{app}} A(h_{\text{s}}'). \qquad (15)$$

The first term of eqn (15) is the work done by the lateral pressure while swollen chains invade the space above the collapsed chains. In this process, the height h_{s} of swollen chains at this space decreases with increasing the area $A(h_{\text{s}})$ of these chains (and vice versa), provided that a constant pressure Π_{app} is applied to these chains. The second term of eqn (15) is the work done by the applied pressure Π_{app} in this process. $\Pi_\|(\phi)$ is the excess lateral pressure and has the form

$$\frac{\Pi_\|(\phi)h_{\text{s}}}{T} = -\frac{3}{N_{\text{s}}l_{\text{eff}}{}^2} + \left[\frac{1}{2}w_{\text{on}}\Phi_{\text{s on}}{}^2 + w_{\text{int}}\Phi_{\text{s on}}\Phi_{\text{s off}}\right. \\ \left. + \frac{1}{2}w_{\text{off}}\Phi_{\text{s off}}{}^2 + \frac{2}{3}u\Phi_{\text{s on}}{}^3 - \frac{\Pi_{\text{app}}}{T}\right]h_{\text{s}}. \qquad (16)$$

The derivation of eqn (16) is shown in Section S2 in ESI.† The first term of eqn (16) is the entropic elasticity due to the lateral excursion of swollen chains and is significant only when the grafting density of DNA chains is relatively small. N_{s} is the

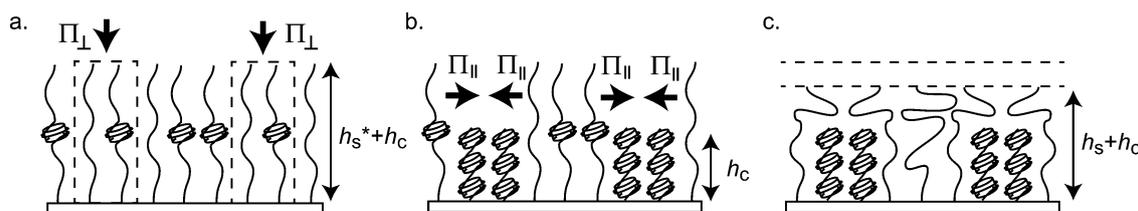

Fig. 2 Two-step process to predict a layer structure: (i) pressure is applied to a fraction of chains in the normal direction to collapse chains (a → b) and then (ii) swollen chains are allowed to diffuse to the space above the collapsed chains (b → c).

number of chain segments (per chain) in the region above the collapsed chains. $\Phi_{\mathrm{s\,on}}$ ($= \sigma\phi N_{\mathrm{s}}n_{\mathrm{his}}/h_{\mathrm{s}}$) and $\Phi_{\mathrm{s\,off}}$ ($= \sigma\phi N_{\mathrm{s}}(1 - n_{\mathrm{his}})/h_{\mathrm{s}}$) in eqn (16) are the concentrations of nucleosomes and vacant DNA chain segments in this region.

The above argument leads to the fact that the work that is necessary to collapse a small fraction $\delta\phi$ of swollen chains has the form $-\dfrac{\mathrm{d}W(\phi)}{\mathrm{d}\phi}\delta\phi$. In a steady state, collapsed chains change to swollen chains with the same rate as the reverse process. This leads to the condition

$$\frac{\mathrm{d}W(\phi)}{\mathrm{d}\phi} = 0. \tag{17}$$

Eqn (17) returns to the Maxwell construction for cases in which DNA brushes show macroscopic lateral phase separations, where $W_{\|}(\phi) = W_{\mathrm{int}}(\phi) = 0$. Eqn (17) is thus a reasonable extension of the Maxwell construction to predict the layered structures of DNA brushes. Eqn (17) corresponds to the minimization of the generalized free energy in the steady state thermodynamics.[31]

The layer structure is more stable than the lateral phase separation when the work $W(\phi)$ is smaller than the work $W_{\perp}(\phi)$. The work $W_{\perp}(\phi)$ has a minimum at $\phi = 0$ (a uniform collapsed brush) or 1 (a uniform swollen brush) because it is a linear function of the fraction ϕ. The lateral phase separation is driven for $W_{\perp}(\phi) = 0$, which is equivalent to the Maxwell construction. We derive the phase diagram of a DNA brush by finding the minimum of the work $W(\phi)$ and $W_{\perp}(\phi)$, see also Section S4 in the ESI.†

2.7 Chain partition

In the layer structure, the segments of swollen chains are located at the interstitial regions between domains of collapsed chains and the space above the collapsed chains. The partition of the chain segments between the two regions is determined by the equality of the chemical potentials of chain segments in the two regions. The chemical potentials μ_{c} of chain segments in the interstitial region between collapsed chains have the form

$$\begin{aligned}\frac{\mu_{\mathrm{c}}}{T}\frac{\sigma N_{\mathrm{c}}}{h_{\mathrm{c}}} = &-\frac{3}{2}\frac{\sigma h_{\mathrm{c}}}{N_{\mathrm{c}}l_{\mathrm{eff}}{}^{2}} + w_{\mathrm{on}}\Phi_{\mathrm{c\,on}}{}^{2} + 2w_{\mathrm{int}}\Phi_{\mathrm{c\,on}}\Phi_{\mathrm{c\,off}} \\ &+ w_{\mathrm{off}}\Phi_{\mathrm{c\,off}}{}^{2} + u\Phi_{\mathrm{c\,on}}{}^{3},\end{aligned} \tag{18}$$

where N_{c} is the number of chain segments (per chain) in this region. $\Phi_{\mathrm{c\,on}}$ ($= \sigma N_{\mathrm{c}}n_{\mathrm{his}}/h_{\mathrm{c}}$) and $\Phi_{\mathrm{c\,off}}$ ($= \sigma N_{\mathrm{c}}(1 - n_{\mathrm{his}})/h_{\mathrm{c}}$) are the concentrations of nucleosomes and vacant chain segments in the region. The chemical potentials μ_{s} of chain segments in the region above the collapsed chains have the form

$$\begin{aligned}\frac{\mu_{\mathrm{s}}}{T}\frac{\sigma\phi N_{\mathrm{s}}}{h_{\mathrm{s}}} = &-\frac{3}{2}\frac{\phi\sigma h_{\mathrm{s}}}{N_{\mathrm{s}}l_{\mathrm{eff}}{}^{2}} - 3\frac{1-\phi}{N_{\mathrm{s}}h_{\mathrm{s}}l_{\mathrm{eff}}{}^{2}} + w_{\mathrm{on}}\Phi_{\mathrm{s\,on}}{}^{2} + 2w_{\mathrm{int}}\Phi_{\mathrm{s\,on}}\Phi_{\mathrm{s\,off}} \\ &+ w_{\mathrm{off}}\Phi_{\mathrm{s\,off}}{}^{2} + u\Phi_{\mathrm{s\,on}}{}^{3},\end{aligned} \tag{19}$$

where the second term is the contribution of the entropic elasticity with respect to the lateral excursion of swollen chains

and is zero for $\phi = 1$. The derivation of eqn (18) and (19) are shown in Section S2 in the ESI.†

2.8 Dimensionless parameters

We here reduce the number of parameters by rescaling them with characteristic length and pressure scales and introducing a dimensionless rescaled rate constant. The force balance equation leads to the scales of the brush height h_{Alx} and osmotic pressure Π_{Alx} in the forms

$$h_{\mathrm{Alx}} = N l_{\mathrm{a}}\left(\frac{|w|\sigma}{6 l_{\mathrm{a}}}\right)^{1/3} \tag{20}$$

$$\frac{\Pi_{\mathrm{Alx}}}{T} = \frac{3\sigma}{l_{\mathrm{a}}}\left(\frac{|w|\sigma}{6 l_{\mathrm{a}}}\right)^{1/3}, \tag{21}$$

respectively, where h_{Alx} is the height of the Alexander brush and Π_{Alx} is the pressure that is necessary to compress the Alexander brush by $\sim 1/4$. In eqn (20) and (21), we used a combination w ($= w_{\mathrm{on}} + w_{\mathrm{off}} - 2w_{\mathrm{int}}$) of the 2nd virial coefficients of chromatin–chromatin interactions (including both nucleosomes and vacant DNA segments). In this paper, we mainly treat cases in which the virial coefficient w is negative. The magnitudes of chromatin–chromatin interactions also depend on the nucleosome occupancy, relative to the other two combinations $n_{\pm} = \left(w_{\mathrm{off}} - w_{\mathrm{int}} \pm \sqrt{w_{\mathrm{int}}{}^{2} - w_{\mathrm{on}}w_{\mathrm{off}}}\right)\big/ w$ of the 2nd virial coefficients. The nucleosome occupancy depends on the transcription dynamics and the dynamics of nucleosome assembly/disassembly *via* the rescaled rate constant

$$\eta_{0} = \frac{\lambda_{\mathrm{p}}\rho_{0}\zeta}{\lambda_{\mathrm{his}}c_{0}\xi}. \tag{22}$$

The transcription rate (and the disassembly of nucleosomes) increases relative to the rate of nucleosome assembly with increasing the rescaled rate constant η_{0}. We use the rescaled virial coefficients $\tilde{u} = 4uN\sigma/(3|w|h_{\mathrm{Alx}})$ and $\tilde{\nu} = \nu\sigma N/h_{\mathrm{Alx}}$.

3 Results

3.1 Transcription drives bistability in chromatin structure

To be self-contained, we first treat the stability of uniform phase. The results of this section has been already shown in our previous work.[11] The equality of rates, eqn (6) and (7), leads to the brush height h as a function of the nucleosome occupancy n_{his}. Substituting this relationship into the force balance equation, eqn (10), leads to the nucleosome occupancy and brush height of a uniform DNA brush as functions of applied pressure (see Fig. 3).

For relatively large values of the rescaled rate constant η_{0}, the nucleosome occupancy increases continuously with increasing applied pressure Π_{app} when the applied pressure is smaller than a threshold value Π_{sp1} (see Fig. 3). For larger applied pressure ($\Pi_{\mathrm{sp1}} < \Pi_{\mathrm{app}} < \Pi_{\mathrm{sp2}}$), the nucleosome occupancy has three solutions, where one of the solutions is unstable (shown by broken curves in Fig. 3). The two threshold pressures, Π_{sp1} and Π_{sp2}, thus correspond to the pressures on
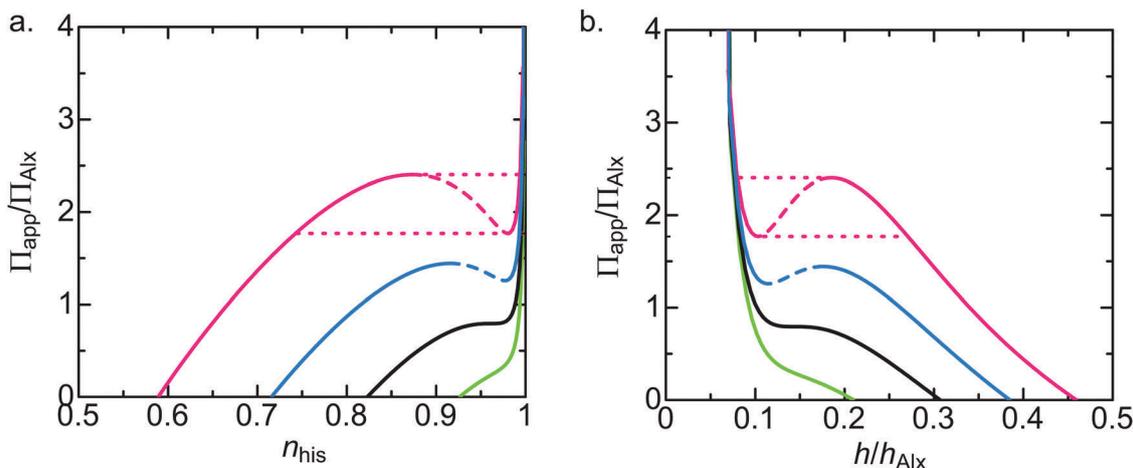
Fig. 3 The nucleosome occupancy n_{his} and rescaled height h/h_{Alx} of a DNA brush is shown as a function of rescaled applied pressure Π_{app}/Π_{Alx} for rescaled rate constants $\eta_0 = 0.2$ (light green), 0.325555 (black), 0.5 (cyan), and 0.8 (magenta). Stable solutions are shown by solid curves and unstable solutions are shown by broken curves. The parameter values used for the calculations are $n_+ = 0.99$, $n_- = -0.1$, $\tilde{u} = 0.002$, $\tilde{\nu} = 0.8$, and $\gamma = 0.7$.

the spinodal curve. This situation is analogous to the van der Waals theory of liquid–gas phase transitions. The bistability implies that the DNA brush shows phase separation at applied pressure Π_{app} between the spinodal pressures. This phase separation results from the instability arising from the fact that nucleosomes are disassembled when RNAP collides with nucleosomes during transcription; the nucleosome occupancy decreases with increasing transcription rate and the transcription rate, in turn, increases with decreasing the nucleosome occupancy because RNAP tends to be localized at the region of smaller local nucleosome concentration (due to the excluded volume interactions between RNAP and nucleosomes). The local concentration of nucleosomes increases with increasing applied pressure. The DNA brush shows phase separation when the transcription rate and the rate of nucleosome assembly balance. When the applied pressure is larger than the second threshold value Π_{sp2}, the nucleosome occupancy increases with increasing applied pressure.

The difference between the two spinodal pressures decreases with decreasing rescaled rate constant η_0. Eventually, the two spinodal pressures become equal at the critical rescaled rate constant η_{0c} (see the black curve in Fig. 3). For smaller values of the rescaled rate constant, the nucleosome occupancy increases monotonically with increasing applied pressure.

3.2 Lateral osmotic pressure stabilizes layer structure

Now we take into account the work done by the lateral pressure $\Pi_{\parallel}$ to predict that DNA brushes stabilize the layer structure. For simplicity, we here treat relatively simple cases in which the grafting density of DNA chains is very large, making the entropic elasticity with respect to lateral excursion of swollen chains negligible (see Section S2 in the ESI†).

An extension of the Maxwell construction that takes into account the work done by the lateral pressure predicts that the layered structure is stabilized in the entire region delineated by the two spinodal curves, Π_{sp1} and Π_{sp2}, for cases in which the
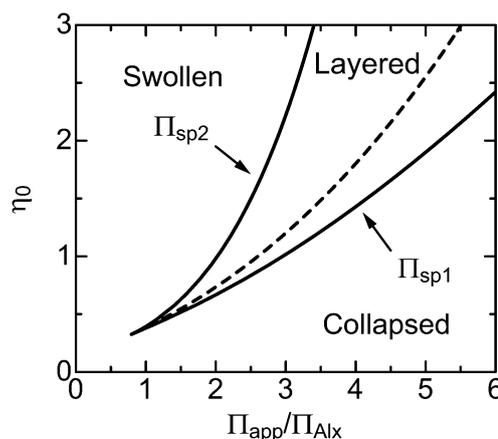

Fig. 4 The phase diagram of DNA brushes is shown as a function of the rescaled rate constant η_0 (defined by eqn (22)) and applied pressure (rescaled by the osmotic pressure Π_{Alx} of the Alexander brush) for cases in which the grafting density is very large $\sigma h_{Alx}^2 \gg 1$ (where the lateral entropic elasticity is negligible). The layered phase is delineated by the two threshold curves, Π_{sp1} and Π_{sp2}. These curves intersect at the critical point $\eta_{0c} = 0.325555$ and $\Pi_c/\Pi_{Alx} = 0.794625$. One phase (either swollen or collapsed) is stable in the exterior of the two curves. The broken curve is the threshold pressure of the lateral phase separation and it is less stable than the layered structure. The values of parameters that are used for the calculations are $n_+ = 0.99$, $n_- = -0.1$, $\tilde{u} = 0.002$, $\tilde{\nu} = 0.8$, and $\gamma = 0.7$.

2nd virial coefficient w is negative (see Fig. 4). The layer structure is thus more stable than lateral phase separation in the entire region of the two-phase coexistent state. This is because the lateral osmotic pressure of swollen chains is relatively large when the grafting density is large and the work done by the lateral osmotic pressure is larger than the work that is necessary to collapse chains. When one increases the applied pressure to a uniform swollen brush, the fraction ϕ of swollen chains in the DNA brush jumps from unity to a smaller value at the threshold pressure Π_{sp1}, similar to first order phase transitions (see Fig. 5). The fraction ϕ then decreases continuously
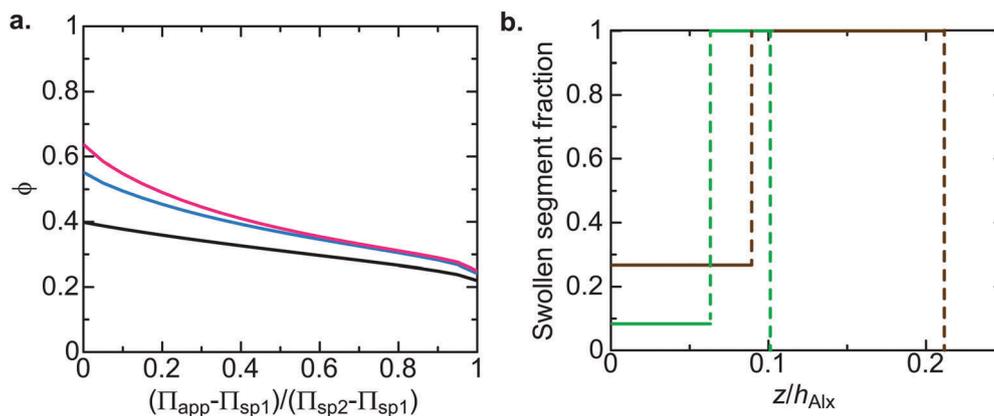
Fig. 5 (a) The fraction ϕ of swollen chains is shown as a function of applied pressure (rescaled by the two spinodal pressures, Π_{sp1} and Π_{sp2}) for $\eta_0 = 1.0$ (black), 2.0 (blue), and 3.0 (red). (b) The fraction of the segments of swollen chains is shown as a function of the distance z/h_{Alx} from the grafting surface for $\eta_0 = 2.0$. We calculated for $\Pi_{app}/\Pi_{Alx} = 2.87$ (brown) and 5.20 (green), which are indeed the threshold pressures, Π_1 and Π_2 (see also the ends of the blue curve in a). The fraction of the segments of swollen chains is $N_c\phi/((1-\phi)N + \phi N_c)$ for $z < h_c$ and 1 for $h_c < z < h_s + h_c$. We used $n_+ = 0.99$, $n_- = -0.1$, $\tilde{u} = 0.002$, $\tilde{\nu} = 0.8$, and $\gamma = 0.7$ for the calculations of both a and b.

with increasing applied pressure. At the second threshold pressure Π_{sp2}, the fraction ϕ jumps to zero, again similar to first order phase transitions. This is in contrast to two-component polymer brushes, where the fraction of polymer components is fixed.

3.3 DNA brushes show tricritical points for small DNA grafting density

The lateral osmotic pressure of swollen chains decreases with decreasing grafting density of the chains. One may think that the layer structure is unstable when the grafting density is small enough. When the distances between swollen chains are relatively large, the entropic elasticity with respect to the lateral excursions of these swollen chains (to the space above collapsed chains) is not negligible and it decreases the osmotic pressure of the swollen chains (see Section 2.6). We here show cases in which swollen chains occupy the space above the collapsed chains without vacancy; the osmotic pressure of these swollen chains stabilizes the collapsed chains below. We predict the phase diagram of the brush by finding the fraction ϕ of swollen chains at the global minimum of the work $W(\phi)$ (see also eqn (17)).

Our theory predicts that a DNA brush shows lateral phase separation, rather than the layer structure, for relatively small values of the rescaled rate constant η_0 (see the green line in Fig. 6). Whether the lateral phase separation is a macroscopic phase separation or a microphase separation depends on the sign of the interfacial tension and is beyond the scope of this paper. The DNA brush shows a lateral phase separation for the rescaled rate constant η_0 that is larger than the critical point (see the filled circle in Fig. 6) and is smaller than the triple point, where the layer structure, the uniform collapsed brush, and the uniform swollen brush coexist (see the intersection of the blue and green curve in Fig. 6). The layer structure is stabilized only for values of the rescaled rate constant η_0 that are larger than the triple point. For larger values of the rescaled rate constant η_0, the DNA brush stabilizes the layer structure at
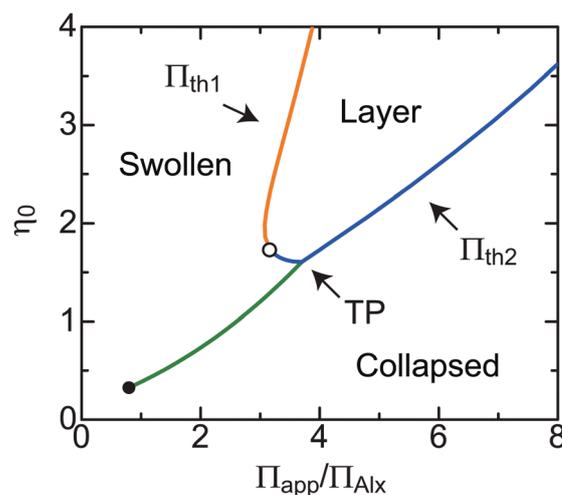

Fig. 6 The phase diagram of a DNA brush is shown as a function of the rescaled rate constant η_0 (defined by eqn (22)) and applied pressure Π_{app} (rescaled by the osmotic pressure Π_{Alx} of Alexander brush) for $\sigma h_{Alx}^2 = 10.0$. The green line shows the applied pressure, at which the DNA brush shows lateral phase separation. The brush shows a critical point (filled circle) at one end of the green line and a triple point at the other end ('TP'). The layer structure is stabilized in the region delineated by the orange and blue curves. The blue curve corresponds to a first order phase transition (with respect to the fraction ϕ of swollen chains) and the orange curve indicates second order phase transitions with respect to the fraction ϕ. The blue curve and the orange curve intersect at the tricritical point (unfilled circle). The values of parameters that are used for the calculations are $n_+ = 0.99$, $n_- = -0.1$, $\tilde{u} = 0.002$, $\tilde{\nu} = 0.8$, and $\gamma = 0.7$. The details of the derivation of this figure is shown in Section S4 in the ESI.†

a threshold applied pressure Π_{th1}, as one increases the applied pressure from a uniform swollen state (see the blue curve in Fig. 7). The fraction ϕ of swollen chains decreases with increasing applied pressure. The layered brush shows transitions to a uniform collapsed brush at the second threshold applied pressure Π_{th2}. The first threshold value Π_{th1} is larger than the spinodal pressure Π_{sp2} and the second threshold value Π_{th2}
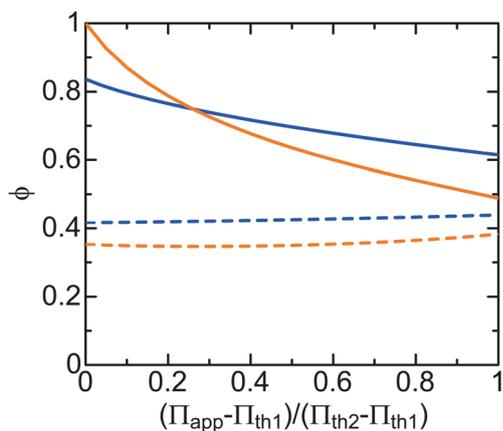
Fig. 7 The fraction ϕ of swollen chains is shown as a function of applied pressure Π_{app} (rescaled by two transition pressures, Π_{th1} and Π_{th2}) for cases in which the grafting density is relatively small $\sigma h_{Alx}^2 = 10.0$. The blue and orange curves show the cases where the brush shows a first order phase transition ($\eta_0 = 1.65$) and a second order phase transition ($\eta_0 = 2.0$) at $\Pi_{app} = \Pi_{th1}$, respectively. We treat cases in which swollen chains fill the space above collapsed chains and this treatment is effective for the values of the fraction ϕ that are larger than the threshold value ϕ_{min} (shown by the broken curve). The values of parameters that are used for the calculations are $n_+ = 0.99$, $n_- = -0.1$, $\tilde{u} = 0.002$, $\tilde{\nu} = 0.8$, and $\gamma = 0.7$.

Fig. 8 The rescaled rate constants η_0 at the triple point (emerald green) and the tricritical point (purple) are shown as functions of the inverse of the grafting density σ^{-1} (rescaled by the brush height of the Alexander brush). The rescaled rate constants η_{0c} at the critical point is shown by the (black) broken curve as a reference. The values of parameters that are used for the calculations are $n_+ = 0.99$, $n_- = -0.1$, $\tilde{u} = 0.002$, $\tilde{\nu} = 0.8$, and $\gamma = 0.7$.

is smaller than the spinodal pressure Π_{sp1}; the layer structure is less stable than the cases in which the grafting density is very large. This is because the lateral osmotic pressure decreases due to the lateral entropic elasticity. These results demonstrate the fact that the lateral osmotic pressure of swollen chains plays an important role in stabilizing the layer structure of DNA brushes.

The fraction ϕ of swollen chains jumps at the first threshold pressure Π_{th1}, analogous to first order phase transitions, for cases in which the rescaled rate constant η_0 is smaller than a threshold value η_{0tri} (see the blue curve in Fig. 6). In contrast, when the rescaled rate constant η_0 is larger than the threshold value η_{0tri}, the fraction ϕ changes continuously at the threshold pressure Π_{th1}, analogous to second order phase transitions (see the orange curve in Fig. 6). The threshold rescaled rate constant η_{0tri} is thus a tricritical point (see the unfilled circle in Fig. 6). At the tricritical point, the first and second derivative of the work $W(\phi)$ with respect to the fraction ϕ of swollen chains is zero and the DNA brush thus shows relatively large fluctuations with respect to the fraction ϕ. This situation may be analogous to the chromatin of embryonic stem cells[3] and is very different from two-component polymer brushes, where the fraction of polymer components is fixed. The large fluctuations are driven by the fact that the lateral osmotic pressure of swollen chains is balanced by the lateral entropic elasticity of these chains. We could not find such tricritical points on the curve of the second threshold pressure Π_{th2} for the values of parameters that were covered in our numerical calculations.

Our theory predicts that DNA brushes show lateral phase separation and tricritical points only for relatively small grafting densities. A natural question is thus to ask how the phase diagram of DNA brushes depends on the grafting density.
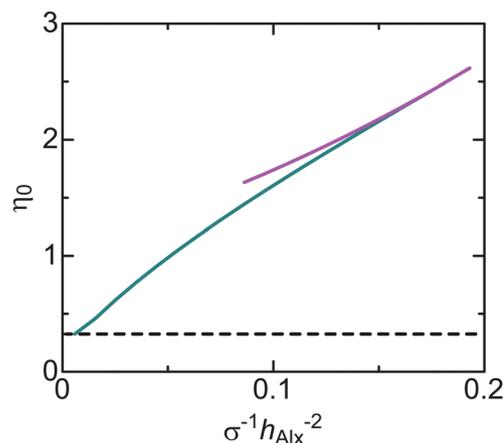
When one decreases the grafting density of a DNA brush from a very large value, the DNA brush starts to show a triple point at a threshold grafting density (see the intersection between the emerald green curve and the black broken curve in Fig. 8). At the threshold grafting density, the triple point is located at the critical point. The lateral phase separation is stabilized for the values of rescaled rate constant η_0 that are smaller than the rescaled rate constant at the triple point (see the emerald green curve in Fig. 8) and are larger than the critical rescaled rate constant η_{0c} (see the black broken curve in Fig. 6). The rescaled rate constant at the triple point increases with decreasing the grafting density, whereas the critical rescaled rate constant is constant. At the second threshold grafting density, DNA brushes start to show a tricritical point (see the purple curve in Fig. 8). The rescaled rate constant at the triple point and the rescaled rate constant at the tricritical point both increase with decreasing the grafting density. These points intersect at the third threshold grafting density. For smaller grafting densities, the transitions from a uniform swollen brush to the layer structure are always of second order.

4 Discussion

Our theory predicts that DNA brushes stabilize a layer structure, where collapsed chains lie at the grafting surface and swollen chains cover the space above the collapsed chains. The bistability of swollen and collapsed chains is due to the instability arising from the fact that nucleosomes are disassembled by RNAP during transcription and the layer structure is stabilized by the lateral osmotic pressure of the swollen chains. When the grafting density is relatively small, the lateral osmotic pressure is suppressed by the entropic elasticity of DNA chains with respect to the lateral excursions of swollen chains. DNA brushes show a tricritical point for a critical rescaled rate constant η_{0tri},

at which the lateral entropic elasticity and lateral osmotic pressure of swollen chains balance. At the tricritical point, DNA brushes show large fluctuations of the fraction ϕ of swollen chains because the fraction ϕ changes with approximately zero mechanical work. The DNA brushes stabilize the layer structure just by increasing applied pressure from the tricritical point. Critical experimental tests of these predictions by using a simple synthetic DNA brush may advance our understanding of the physics of the phase separation and pattern formation of chromatin.

The layer structure is reminiscent of the canonical structure of differentiated cell nuclei and the fluctuations at the tricritical point are reminiscent of the critical fluctuations of chromatin of stem cells. It is tempting to think that our theory captures the essential features of the phase separation and pattern formation of chromatin during differentiation. Experiments have shown that the canonical structure of the nucleus of differentiated cells is stabilized by lamin A/C and LBR proteins, which tether chromatin to nuclear membranes.[36] The situation of tethered chromatin is analogous to the DNA chains of a brush. The canonical structure of differentiated cell nuclei has been predicted by using Monte Carlo simulations assuming that chromatin is composed of a mixture of chain units that already have heterochromatin-like or euchromatin-like mechanical properties[32] or have corresponding different activities (treated by different effective temperatures).[33] These simulations predict that the canonical structure is stabilized even without the tethering of chromatin to nuclear membranes, in contrast to the forementioned experiments. The canonical structure was also predicted by assuming that the two types of chain units are in different solvent conditions[34] or have different mobilities in a pulsating container.[35] These simulations predict that the canonical structure is stabilized only when hetero-chromatin is specifically tethered to nuclear membranes, in agreement with forementioned experiments. In contrast to these simulations, our theory predicts that the phase separation of a DNA brush is driven even for cases in which each DNA chain in the brush is homogeneous and the canonical structure is stabilized even when both euchromatin and hetero-chromatin are non-specifically tethered to the nuclear membranes.

We have used an extension of the Maxwell construction to predict that DNA brushes stabilize the layer structure. Steady state thermodynamics states that the work done to change a non-equilibrium steady state to another steady state is the effective free energy difference between these states, when so-called 'house-keeping' heat is subtracted. However, there is no general theory that predicts the binodal curve of the phase separation of non-equilibrium systems. Indeed, a comparison between theory and simulation predicts that the binodal curve that is predicted by using the Maxwell construction deviates from simulations for interacting active Brownian particles,[37] whereas an analytical theory that treats the active nature of these particles by using effective temperatures shows that the common tangent method is effective when the particles are dilute enough.[38]

Defining pressure is not trivial in these systems because the active motion of these particles directly contributes to the pressure.

In contrast, the osmotic pressure in a DNA brush is generated by the entropic elasticity of DNA chains and the interactions between DNA chain segments when the concentration of RNAP is dilute enough; the active motion of RNAP during transcription contributes to the osmotic pressure only indirectly *via* the nucleosome occupancy. Our theory assumes that the mechanical work to change a small fraction of DNA chains from the swollen state to the collapsed state (and *vice versa*) must be zero for the two states to coexist, see eqn (17). This is probably true even for a non-equilibrium steady state as long as DNA chains can take either of the two states because there is no net flow from one state to the other. The Maxwell construction might thus be effective to treat the phase separation of a DNA brush to the first approximation. It is of interest to find a general theoretical framework that predicts phase separation in non-equilibrium steady states.

References

1 H. Schiessel, The physics of chromatin, *J. Phys.: Condens. Matter*, 2003, **15**, R699–R774.

2 K. Luger, A. W. Mäder, R. K. Richmond, D. F. Sargent and T. J. Richmond, Crystal structure of the nucleosome core particle at 2.8 Å resolution, *Nature*, 1997, **389**, 251–260.

3 S. Talwar, A. Kumar, M. Rao, G. I. Menon and G. V. Shivashankar, Correlated Spatio-Temporal Fluctuations in Chromatin Compaction States Characterize Stem Cells, *Biophys. J.*, 2013, **104**, 553–564.

4 S. S. Daube, D. Bracha, A. Buxboim and R. H. Bar-Ziv, Compartmentalization by directional gene expression, *Proc. Natl. Acad. Sci. U. S. A.*, 2010, **107**, 2836–2841.

5 A. Buxboim, S. S. Daube and R. Bar-Ziv, Synthetic Gene Brushes: a Structure–Function Relationship, *Mol. Syst. Biol.*, 2008, **4**, 181.

6 D. Bracha, E. Karzbrun, S. S. Daube and R. H. Bar-Ziv, Emergent Properties of Dense DNA Phases toward Artificial Biosystems on a Surface, *Acc. Chem. Res.*, 2014, **47**, 1912–1921.

7 D. Bracha, E. Karzbrun, G. Shemer, P. A. Pincus and R. H. Bar-Ziv, Entropy-driven collective interactions in DNA brushes on a biochip, *Proc. Natl. Acad. Sci. U. S. A.*, 2013, **110**, 4534–4538.

8 M. Lindner, G. Nir, S. Medalion, H. R. C. Dietrich, Y. Rabin and Y. Garini, Force-free measurements of the conformation of DNA molecules tethered to a wall, *Phys. Rev. E: Stat., Nonlinear, Soft Matter Phys.*, 2011, **83**, 011916.

9 T. Yamamoto and S. A. Safran, Transcription rates in DNA brushes, *Soft Matter*, 2015, **11**, 3017–3021.

10 V. Nikolov, R. Lipowsky and R. Dimova, Behavior of Giant Vesicles with Anchored DNA Molecules, *Biophys. J.*, 2007, **92**, 4356–4368.

11 T. Yamamoto and H. Schiessel, Transcription driven phase separation in chromatin brush, *Langmuir*, 2016, **32**, 3036–3044.

12 S. A. Safran, *Statistical Thermodynamics of Surfaces, Interfaces, and Membranes*, Westview, CO, 2003.

13 F. Mühlbacher, C. Holm and H. Schiessel, Controlled DNA compaction within chromatin: the tail-bridging effect, *Europhys. Lett.*, 2006, **73**, 135–141.

14 J. Widom, Physicochemical Studies of the Folding of the 100 Å Nucleosome Filament into the 300 Å Filament: Cation Dependence, *J. Mol. Biol.*, 1986, **190**, 411–424.

15 S. Mangenot, A. Leforestier, P. Vachette, D. Durand and F. Livolant, Salt-Induced Conformation and Interaction Changes of Nucleosome Core Particles, *Biophys. J.*, 2002, **82**, 345–356.

16 S. Mangenot, E. Raspaud, C. Tribet, L. Belloni and F. Livolant, Interactions between isolated nucleosome core particles: a tail-bridging effect?, *Eur. Phys. J. E: Soft Matter Biol. Phys.*, 2002, **7**, 221–231.

17 R. Blossey and H. Schiessel, The dynamics of the nucleosome: thermal effects, external forces and ATP, *FEBS J.*, 2011, **278**, 3619–3632.

18 I. M. Kulić and H. Schiessel, Chromatin Dynamics: Nucleosomes go Mobile through Twist Defects, *Phys. Rev. Lett.*, 2003, **91**, 148103.

19 I. M. Kulić and H. Schiessel, Nucleosome repositioning via loop formation, *Biophys. J.*, 2003, **84**, 3197–3211.

20 L. Bintu, M. Kopaczynska, C. Hodges, L. Lubkowska, M. Kashlev and C. Bustamante, The elongation rate of RNA polymerase determines the fate of transcribed nucleosomes, *Nat. Struct. Mol. Biol.*, 2011, **18**, 1394–1399.

21 B. ten Heggeler-Bordier, S. Muller, M. Monestier and W. Wahli, An Immuno-electron Microscopical Analysis of Transcribing Multinucleosomal Templates: What Happens to the Histones?, *J. Mol. Biol.*, 2000, **299**, 853–858.

22 R. Bruinsma, A. Y. Grosberg, Y. Rabin and A. Zidovska, Chromatin Hydrodynamics, *Biophys. J.*, 2014, **106**, 1871–1881.

23 R. C. van Lehn and A. Alexander-Katz, Lateral phase separation of mixed polymer brushes physisorbed on planar substrates, *J. Chem. Phys.*, 2011, **135**, 141106.

24 J. F. Marko and T. A. Witten, Phase separation in a Grafted Polymer Layer, *Phys. Rev. Lett.*, 1991, **66**, 1541–1544.

25 M. Müller, Phase diagram of a mixed polymer brush, *Phys. Rev. E: Stat., Nonlinear, Soft Matter Phys.*, 2002, **65**, 030802.

26 S. Minko, M. Müller, D. Usov, A. Scholl, C. Foeck and M. Stamm, Lateral versus Perpendicular Segregation in Mixed Polymer Brushes, *Phys. Rev. Lett.*, 2002, **88**, 035502.

27 S. Komura and S. A. Safran, Scaling theory of mixed amphiphile monolayers, *Eur. Phys. J. E: Soft Matter Biol. Phys.*, 2001, **5**, 337–351.

28 N. Kaplan, I. K. Moore, Y. Fondufe-Mittendorf, A. J. Gossett, D. Tillo, Y. Field, E. M. LeProust, T. R. Hughes, J. D. Lieb, J. Widom and E. Segal, The DNA-encoded nucleosome organization of a eukaryotic genome, *Nature*, 2009, **458**, 362–366.

29 J. K. Marko and E. D. Siggia, Stretching DNA, *Macromolecules*, 1995, **28**, 8759–8770.

30 J. C. Maxwell, On the dynamical evidence of the molecular constitution of bodies, *Nature*, 1875, **11**, 357–359.

31 T. Hatano and S. Sasa, Steady-State Thermodynamics of Langevin Systems, *Phys. Rev. Lett.*, 2001, **86**, 3463–3466.

32 P. R. Cook and D. Marenduzzo, Entropic organization of interphase chromosomes, *J. Cell Biol.*, 2009, **186**, 825–834.

33 N. Ganai, S. Sengupta and G. I. Menon, Chromosome positioning from activity-based segregation, *Nucleic Acids Res.*, 2014, **42**, 4145–4159.

34 H. Jerabek and D. W. Heerman, How chromatin looping and nuclear envelope attachment affect genome organization in eukaryotic cell nuclei, *Int. Rev. Cell Mol. Biol.*, 2014, **307**, 351–381.

35 A. Awazu, Nuclear dynamical deformation induced hetero- and euchromatin positioning, *Phys. Rev. E: Stat., Nonlinear, Soft Matter Phys.*, 2015, **92**, 032709.

36 I. Solovei, A. S. Wang, K. Thanisch, C. S. Schmidt, S. Krebs, M. Zwerger, T. V. Cohen, D. Devys, R. Foisner, L. Peichl, H. Herrmann, H. Blum, D. Engelkamp, C. L. Stewart, H. Leonhardt and B. Joffe, *Cell*, 2013, **152**, 584–598.

37 A. P. Solon, J. Stenhammar, R. Wittkowski, M. Kardar, Y. Kafri, M. E. Cates and J. Tailleur, Pressure and Phase Equilibria in Interacting Active Brownian Spheres, *Phys. Rev. Lett.*, 2015, **114**, 198301.

38 A. Y. Grosberg and J. F. Joanny, Nonequilibrium statistical mechanics of mixture of particles in contact with different thermostats, *Phys. Rev. E: Stat., Nonlinear, Soft Matter Phys.*, 2015, **92**, 032118.